Structural characterization of N-acyl-homoserine lactones from bacterial quorum sensing using LC–MS/MS analyses after Paternò-Büchi derivatization in solution

Clarisse Gosset-Erard, Guanghui Han, Dimitra Kyrko, Amandine Hueber, Bastien Nay, Véronique Eparvier, David Touboul

Structural characterization of *N*-acyl-homoserine lactones from bacterial quorum sensing using LC-MS/MS analyses after Paternò-Büchi derivatization in solution

Clarisse Gosset-Erard[1], Guanghui Han[2], Dimitra Kyrko[1], Amandine Hueber[1], Bastien Nay[2], Véronique Eparvier[1], David Touboul[1,3]*

1 – Université Paris-Saclay, CNRS, Institut de Chimie des Substances Naturelles, UPR 2301, 91198 Gif-sur-Yvette, France.
2 – Laboratoire de Synthèse Organique (LSO), CNRS UMR 7652, Ecole Polytechnique, ENSTA, Institut Polytechnique de Paris, 91128 Palaiseau, France.
3 – Laboratoire de Chimie Moléculaire (LCM), CNRS UMR 9168, Ecole Polytechnique, Institut Polytechnique de Paris, 91128 Palaiseau, France.

***Correspondence should be addressed to Dr. David Touboul (david.touboul@cnrs.fr)**

Other authors e-mail addresses (in order): clarisse.gosseterard.pro@gmail.com; guanghui.han@polytechnique.edu; dimitra.kyrko@gmail.com; hueberamandine94@gmail.com; bastien.nay@polytechnique.edu; veronique.eparvier@cnrs.fr

Authors 16-digit ORCID (in order) : 0000-0001-8285-8438; Not applicable; Not applicable; Not applicable; Not applicable; 0000-0002-1209-1830; 0000-0002-2954-0866; 0000-0003-2751-774X

Abstract: The bacterial quorum sensing is a chemical language allowing bacteria to interact through the excretion of molecules called auto-inducers, like *N*-acyl-homoserine lactones (AHLs) produced by Gram-negative *Burkholderia* and *Paraburkholderia* bacteria known as opportunistic pathogens. The AHLs differ in their acyl-chain length and may be modified by a 3-oxo or 3-hydroxy substituent, or C=C double bonds at different positions. As the bacterial signal specificity depends on all of these chemical features, their structural characterization is essential to have a better understanding of the population regulation and virulence phenomenon. This study aimed at enabling the localization of the C=C double bond on such specialized metabolites while using significantly low amounts of biological material. The approach is based on LC-MS/MS analyses of bacterial extracts after in-solution derivatization by a photochemical Paternò-Büchi reaction, leading to the formation of an oxetane ring and subsequently to specific fragmentations when performing MS/MS experiments. The in-solution derivatization of AHLs was optimized on several standards, and then the matrix effect of bacterial extracts on the derivatization was assessed. As a proof of concept, the optimized conditions were applied to a bacterial extract enabling the localization of C=C bonds on unsaturated AHLs.

Keywords: structural characterization; *N*-acyl-homoserine lactones; tandem mass spectrometry; Paternò-Büchi derivatization; liquid chromatography; double bond localization

Statements and Declarations: This work was supported by a CHARM$_3$AT LabEx funding (postdoctoral fellowship of C. Gosset-Erard) and by the French ANR program (ANR-20-CE29-001). The authors declare that they have no known competing interests or personal relationships that could have appeared to influence the work reported in this paper.

1. Introduction

Quorum sensing is a widespread and well-known cell density-dependent mechanism, which allows prokaryotes to synchronize their metabolic and physiological activities at high cell concentrations [1]. Quorum sensing system relies on the "sensing" of molecular indicators of bacterial densities. At a low cell density, these compounds, named autoinducers (AIs), are released in small amounts in the nearby environment of bacterial cells [2]. The concentration of AIs in the environment increases concomitantly with the cell concentration and induces intracellular signaling cascades in targeted cells at a certain threshold of detection [3]. These mechanisms lead to deep modifications of gene expression and large phenotypic transformations [4]. For some particular opportunistic human pathogens, these AI molecules regulate the expression of various virulence genes [5] and are involved in the bacterial antibiotic resistance and biofilm formation [6]. The characterization of AIs is therefore critical in a particularly alarming context of infectious diseases surge.

Species of the *Burkholderia* and *Paraburkholderia* genera are Gram-negative bacteria found in diverse environment niches. They are mainly non-pathogenic and plant-benefical-environment species [7–9]. However, some of these bacteria have been described as opportunistic pathogens for humans [10], including the *Burkholderia cepacia* complex that can cause life-threatening infections in immunodeficient patients [11]. The quorum sensing mechanism in *Burkholderia* and *Paraburkholderia* species, as in many Gram-negative bacteria [12], is based on *N*-acyl homoserine lactones (AHLs) [6]. These well-described hydrophobic AIs are composed of a lactone ring linked to a fatty acid residue, with variations in acyl-chain length (generally from C4 to C18) and different oxygenated functions like 3-oxo or 3-hydroxy substituents, as well as C=C double bonds at various positions on the carbon backbone chain (Fig. 1a) [13–15]. Fine structural characterization of AHLs is crucial for understanding population regulation and virulence as signal specificity depends on all of these features [16]. Indeed, the position of the double bonds, and all the other structural differences, could have an impact on the bacterial signal, since AHLs are detected by specific receptors. While tandem mass spectrometry (MS/MS) readily provides information on acyl-chain length and degrees of unsaturation [17], pinpointing C=C double bonds remains challenging due to limitations in classical fragmentation methods like Collision Induced Dissociation (CID) [18].

Alternative fragmentation methods have been developed to localize C=C bonds on lipid acyl chains, mostly on phospholipids, such as Ozone Induced Dissociation (OzID) [19] and Ultra-Violet Photodissociation (UVPD) [20], but these methods require instrumental modifications. Another approach involves the derivatization of C=C bonds using Paternò-Büchi reaction, a photochemical [2+2] cycloaddition between a ketone and an olefin resulting in the formation of an oxetane ring (Fig. 1b) [21]. As demonstrated on phospholipids, this reaction enables the localization of C=C double bonds through CID fragmentation of the oxetane rings, generating specific retro-Paternò-Büchi fragments ($^{X}F_{O}$ and $^{X}F_{A}$, Fig. 1b). Additionally, Paternò-Büchi derivatization enhances lipid ionization, particularly when reagents bear a functional group with a high proton affinity [22].

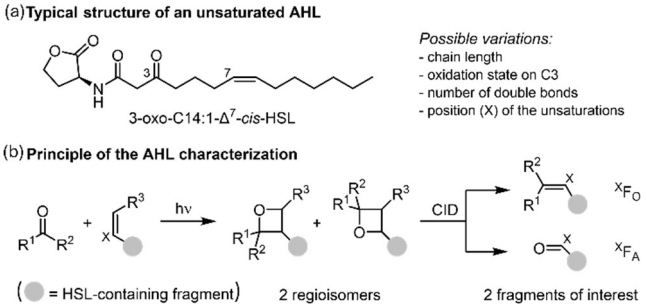

Fig. 1 (a) Typical structure of an unsaturated AHL and (b) principle of this AHL characterization by the Paternò-Büchi derivatization. The structure of the two fragments of interest depends on the position of the unsaturation (X) and contains either an aldehyde ($^{X}F_{A}$) or an olefin ($^{X}F_{O}$). The mechanism of the Paternò-Büchi reaction is available in Fig. S1.

To our knowledge, none of these methods, including Paternò-Büchi derivatization, has been used on AHLs to localize C=C double bonds on the acyl chain. This study aimed to optimize the Paternò-Büchi derivatization in solution for a better structural characterization of AHLs, especially in determining double bond positions. The optimized method was then applied to highly complex bacterial extracts from several strains of *Burkholderia* and *Paraburkholderia* species to evaluate the matrix influence and as a proof of concept towards the determination of bacterial signatures.

2. Material and methods

2.1. Chemicals and standards

Unless specified, all chemicals used were of analytical grade or high purity. Ultra-pure water was obtained from Direct-Q3® water purification system (Merck Millipore, Amsterdam, The Netherlands). Acetonitrile (ACN), methanol (MeOH), isopropanol (IPA) and ethanol (EtOH) were purchased from Carlo Ebra (Val-de-Reuil, France). Technical grade ethyl acetate was purchased from ThermoFisher Scientific (Courtaboeuf, France). Potato dextrose agar was purchased from Condalab (Madrid, Spain). 2-acetylpyridine (APy), 2'-4'-5'-trifluoroacetophenone (TriFAP) and *N*-3-oxo-octanoyl-L-homoserine lactone (3-oxo-C8:0-HSL) were purchased from Sigma Aldrich (Saint-Quentin Fallavier, France). *N*-*cis*-octadec-9Z-enoyl-L-homoserine lactone (C18:1-Δ9-*cis*-HSL), *N*-3-oxo-tetradec-7(*Z*)-enoyl-L-homoserine lactone (3-oxo-C14:1-Δ7-*cis*-HSL), *N*-3-oxo-hexadec-11(*Z*)-enoyl-L-homoserine lactone (3-oxo-C16:1-Δ11-*cis*-HSL) and *N*-*cis*-tetradec-9*Z*-enoyl-L-homoserine lactone (C14:1-Δ9-*cis*-HSL) were purchased from Cayman Chemicals Company (Ann Arbor, MI, USA). C18:1-Δ9-*trans*-HSL, C18:2-Δ9,12-*cis*-HSL and C18:3-Δ9,12,15-*cis*-HSL standards were synthesized from L-homoserine lactone, available from L-methionine [23] (Fig. S2, S3 and S4). 3-oxo-C8:0-HSL, C18:1-Δ9-*cis*-HSL, C18:1-Δ9-*trans*-HSL, C18:2-Δ9,12-*cis*-HSL, C18:3-Δ9,12,15-*cis*-HSL, 3-oxo-C14:1-Δ7-*cis*-HSL, 3-oxo-C16:1-Δ11-*cis*-HSL and C14:1-Δ9-*cis*-HSL were dissolved at 2.5 mM in ACN and store at -20 °C. APy and TriFAP were diluted at 0.5 M in MeOH and stored at room temperature.

2.2. Biological samples, extraction and sample preparation

Two bacterial strains of *Burkholderia* and *Paraburkholderia* genus were used in this study: *Burkholderia* sp. BSNB-0181 and *Paraburkholderia tropica* BSNB-0562 strains isolated from plant and termite holobionts [24, 25] (APA authorization : ABSCH-IRCC-FR-248781-1 and ABSCH-IRCC-FR-248782-1). All strains were maintained at −80 °C in H_2O/glycerol mixture and referenced in the "Strain library" of the Institut de Chimie des Substances Naturelles. Each bacterial strain was cultured on potato dextrose agar in 3 Petri dishes for one week at 28°C. Then, solid-liquid extractions were performed in 200 mL of ethyl acetate while shaking at 80 rpm for 24 hours at room temperature on a TR-250 shaker (Infors HT, Massy, France). The extracts were filtered on paper filters and washed with 200 mL of water. The organic phase was evaporated to dryness using a SyncorePlus Analyst evaporator (Büchi, Villebon-sur-Yvette, France), then dissolved in MeOH before being filtered through a 0.2 µm pore-size polytetrafluoroethylene filter (Interchim, Montluçon, France) previously washed with MeOH. Finally, extracts were evaporated to dryness with a Hei-VAP Value rotary evaporator (Heidolph, Modeville, France). An extract of the culture media without microorganisms was also

conducted. Final crude extracts were dissolved in MeOH at 10 mg.mL^{-1}, and diluted in ACN to a final concentration of 1 mg.mL^{-1}.

2.3. Optimization of the Paternò-Büchi derivatization in solution

2.3.1. Paternò-Büchi derivatization

For the reaction optimization, several parameters were evaluated through a full-factorial design of experiments (DOE): the solvent (MeOH, EtOH, IPA, ACN), the reagent (APy, TriFAP), the UV wavelength (254 nm, 365 nm) and the AHL/reagent molar ratio (1/50, 1/100).

Reaction solutions containing 3-oxo-C8-HSL (100 µM), C18:1-Δ^{9}-*cis*-HSL (100 µM) and the reagent (5 or 10 mM) were prepared in solvent previously degassed using an Ultrasonic Cleaner USC-T (WVR, Rosny-sous-Bois, France) for 5 minutes to prevent side reactions with dissolved O_2 [26]. Solutions were poured into custom-made quartz tubes (0.4 cm ID, 0.6 cm OD) placed parallel to an Analytica Jena UV Pen-Ray lamp at 254 nm (> 2800 microwatt.cm^{-2} at 1" distance) or 365 nm (> 850 microwatt.cm^{-2} at 1" distance) (respectively 90-0012-01 or 90-0079-01 references from Eurobio Scientific, Les Ulis, France) previously heated for 5 min. The UV lamp was about 1.0-1.5 cm away from the quartz tube. After a 15-minute UV exposure, samples were collected in aluminum foil-covered vials to prevent degradation and diluted in MeOH to a final concentration of 2.5 µM per AHL standard prior LC-MS/MS analysis.

2.3.2. Kinetic study

A kinetic study was performed on C18:1-Δ9-*cis*-HSL using optimized solvent, reagent, UV wavelength and AHL/reagent ratio to optimize the reaction time. Samples were prepared in triplicate and collected at different UV-exposure times between 0 s and 60 min. Samples were poured in aluminum foil-covered vials and diluted at 2.5 µM in methanol prior LC-MS/MS analysis.

2.3.3. Stability study

Two stability studies were performed to assess storage conditions: one at 6 °C and the other with freeze/thaw (− 20 °C/6 °C) cycles. For the 6 °C stability, samples underwent repeated LC-MS/MS analyses for 38 h to simulate extended analysis sequence. For the freeze/thaw stability, samples underwent several-day storage at − 20°C, followed by a 2-hour thawing period at 6°C before being re-stocked at − 20°C, mimicking samples requiring multiple re-analyses. All samples, derivatized in triplicate under optimized conditions, were collected in aluminum foil-covered vials and diluted at 2.5 µM in MeOH.

2.3.4. Application to *Z/E* stereoisomers and AHLs containing several double bonds

Paternò-Büchi reactions were performed in solution on C18:1-Δ9-*trans*-HSL, C18:1-Δ9,12-*cis*-HSL and C18:1-Δ9,12,15-*cis*-HSL at 100 µM to ensure that the optimized conditions would also be successful on AHLs with multiple unsaturations and both *Z/E* configuration.

2.4. Liquid chromatography-tandem mass spectrometry (LC-MS/MS)

LC-MS/MS analyses were performed on a 1260 Infinity II liquid chromatography (Agilent Technologies, Massy, France) hyphenated to a 6546 Q-TOF mass spectrometer (Agilent Technologies, Massy, France) equipped with a Dual Jet ESI ion source (Agilent Technologies, Massy, France) and operated by MassHunter software (Agilent Technologies, Massy, France). A volume of 5 µL of standard solution or

bacterial extracts at 1 mg.mL^{-1} was injected on a Accucore RP column (100 mm × 2.1 mm, 2.6 µm) from Thermo Fisher Scientific (Courtaboeuf, France) heated at 50 °C. A mobile phase gradient with 0.1 % formic acid in ultrapure water (A) and acetonitrile (B) was used at a flow rate of 0.4 mL.min^{-1}. For the optimization of the Paternò-Büchi conditions, the following gradient was used: 0.0-1.0 min (30-75 %B), 1.0-3.0 min (75-80 %B), 3.0-3.5 min (80-100 %B), 3.5-7.0 min (100 %B), 7.0-7.5 min (100-30 %B) and 7.5-10.0 min (30 %B). For bacterial extracts analysis, the following gradient was used: 0.0-12.0 min (5-100 %B), 12.0-16.0 min (100 %B), 16.0-16.5 min (100-5 %B) and 16.5-20.0 min (5 %B). MS was performed in ion positive mode over the 90-1700 *m/z* range, with a scan rate of 10 spectra/s. Instrument parameters were set as follows: drying gas at 325 °C and 10 L.min^{-1}, nebulizer at 30 psi, sheath gas at 350 °C and 10 L.min^{-1}, capillary voltage at 3500 V, nozzle voltage at 500 V, fragmentor at 110 V, skimmer at 45 V and octopole RF frequency at 750 Hz. For the optimization of the Paternò-Büchi conditions, targeted MS/MS using CID fragmentation mode was performed with a MS/MS rate of 4 spectra/sec and a collision energy fixed at 20 eV. For the assessment of the matrix effect and for the analyses of bacterial extracts, data-dependent MS/MS was performed using CID fragmentation mode with a collision energy fixed at 20 eV, a maximum 4 precursors per cycle at a MS/MS rate of 4 spectra/sec, an isolation window of 1.3 amu and an active exclusion of 0.02 min after 1 spectrum.

2.5. Application to bacterial extracts

2.5.1. Estimation of the AHL content

Prior derivatization, AHLs from bacterial extracts at 1 mg.mL^{-1} were quickly annotated from LC-MS/MS analyses. Data processing was performed with MZmine 3 [27] and a molecular network was then calculated and visualized using MetGem software (version 1.4.1) [28, 29]. All parameters used for both software are detailed in Supplementary Information (section 3). The AHLS cluster was localized from the loss of the lactone moiety (product ion at *m/z* 102.0550) [30]. AHLs were annotated from this cluster by comparison of experimental $[M_{AHL}+H]^+$ *m/z* values with a homemade database (Table S1) and retention times (when standards were available). The overall AHL concentration was roughly estimated from LC-MS/MS analyses.

2.5.2. Adaptation of the Paternò-Büchi derivatization to the bacterial extracts matrix

The matrix effect on the ionization efficiency and on the Paternò-Büchi derivatization were assessed following the methods developed by Rebane *et al.* [31]. Briefly, two spiking methods were employed to evaluate the ESI matrix effect and the derivatization matrix effect simultaneously. On one hand, the overall matrix effect ($ME\%^*$) was determined using the post-extraction spike method, where a derivatized standard solution is compared with a bacterial extract spiked with standards before derivatization (Equation 1). On the other hand, the ESI matrix effect ($dME\%$) was determined using the post-derivatization spike method, where a derivatized standard solution is compared with a derivatized bacterial extract spiked with derivatized standards (Equation 2). The relative yield of the Paternò-Büchi derivatization (Y_{rel}^{PB}) was obtained from Equation 3.

$$ME\%^* = \frac{A^*_{matrix}}{A_{STD}} * 100 \quad (1)$$

$$dME\% = \frac{A_{matrix}}{A_{STD}} * 100 \quad (2)$$

$$Y_{rel}^{PB} = \frac{\%ME^*}{\%dME} * 100 \quad (3)$$

With A^*_{matrix} and A_{matrix} the LC-MS peak areas of the Paternò-Büchi products respectively from the post-extraction spike and the post-derivatization spike methods, A_{STD} the peak area of the Paternò-Büchi products from the standard solution.

Six AHLs (C14:1-Δ9-*cis*-HSL, 3-oxo-C14:1-Δ7-*cis*-HSL, 3-oxo-C16:1-Δ11-*cis*-HSL, C18:1-Δ9-*cis*-HSL, C18:2-Δ9,12-*cis*-HSL and C18:3-Δ9,12,15-*cis*-HSL) were mixed in the spiking solution. Several combinations of AHL concentrations (2.5 µM and 25 µM for each AHL) and APy concentrations (1.5 mM, 15 mM and 150 mM) were used for Paternò-Büchi derivatizations. Prior LC-MS/MS analysis, all solutions were diluted to the same concentration of underivatized analytes. The bacterial extract used for this study was from the *Burkholderia* sp. BSNB-0181 strain as no unsaturated AHL was detected by LC-MS/MS.

Derivatization of the *Paraburkholderia tropica* BSNB-0562 strain bacterial extract (1 mg.mL^{-1}) was performed in newly optimized conditions. After derivatization, samples were collected in aluminum foil-covered vials and directly analyzed by LC-MS/MS.

2.6.3. Localization of AHL double bonds

LC-MS/MS data of derivatized *Paraburkholderia tropica* bacterial extract were manually interpreted using Qualitative Mass Hunter (Agilent Technologies, Massy, France). The focus was put on the unsaturated AHLs previously annotated in the molecular network. The identification of the Paternò-Büchi products was based on the exact $[M_{AHL}+M_{reagent}+H]^+$ *m/z* values. The first double bond was localized from the theoretical fragments of the oxetane rings [22] (Table S2), and in case of several double bonds, the other positions were determined based on the difference of 40 amu between fragments of the same series.

3. Results and discussion

3.1. Localization of the C=C bonds

Before optimizing the derivatization conditions, it was crucial to check the successful CID fragmentation of the oxetane rings for the two Paternò-Büchi products with both 2',4',5'-trifluoroacetophenone (TriFAP) and 2-acetylpyridine (APy). Theoretically, CID fragmentation will lead to two specific fragments containing the homoserine lactone moiety, $^{X}F_O$ and $^{X}F_A$ arising from each regioisomer of the Paternò-Büchi products (where X corresponds to the double bond position in the initial AHL, fragment F_O contains an olefin, and fragment F_A contains an aldehyde) (Fig. 1b). [21]

When using TriFAP as a reagent in presence of C18:1-Δ^9-*cis*-HSL, the Paternò-Büchi products were detected at m/z_{theo} 540.3295 as expected, but at a very low intensity. Nevertheless, no theoretical oxetane ring fragments (m/z_{theo} 398.1938 and m/z_{theo} 256.1543) [22] were detected after CID experiments (Fig. S5). This may be due to the low ionization efficiency of the TriFAP-derived fragment.On the other hand, APy allowed to generate the Paternò-Büchi products of C18:1-Δ^9-*cis*-HSL at m/z_{exp} 487.3540 (Δ_{error} = 2.1 ppm) and the characteretic CID fragments $^{9}F_A$ and $^{9}F_O$ at m/z_{exp} 256.1541 (Δ_{error} = 0.8 ppm) and m/z_{exp} 345,.2172 (Δ_{error} = 0.3 ppm), respectively (Fig. 2). Moreover, the complementary fragment ions at m/z_{exp} 232.2061 (Δ_{error} = 0.4 ppm) and m/z_{exp} 244.1700 (Δ_{error} = 1.6 ppm) were also detected confirming the unambiguous C=C localization. The ion at m/z_{exp} 155.1075 (Δ_{error} = 5.2 ppm) is coming from the ion at m/z_{exp} 256.1541 (Δ_{error} = 0.8 ppm) resulting from the fragmentation of the amide bound whereas m/z_{exp} 122.0601 (Δ_{error} = 0.8 ppm) is originating from a gas-phase retro-Paternò-Büchi reaction leading to the formation the protonated APy. Fragmentation mechanisms of both regioisomers are available in Fig. S6 and the energy resolved mass spectrometry

breakdown curve of the C18:1-Δ9-*cis*-HSL Paternò-Büchi products is available in Fig. S7 allowing to determine the optimized CID energy for the structural characterization of derivatized C18 AHLs. Thusonly APy will be employed as reagent for the next experiments.

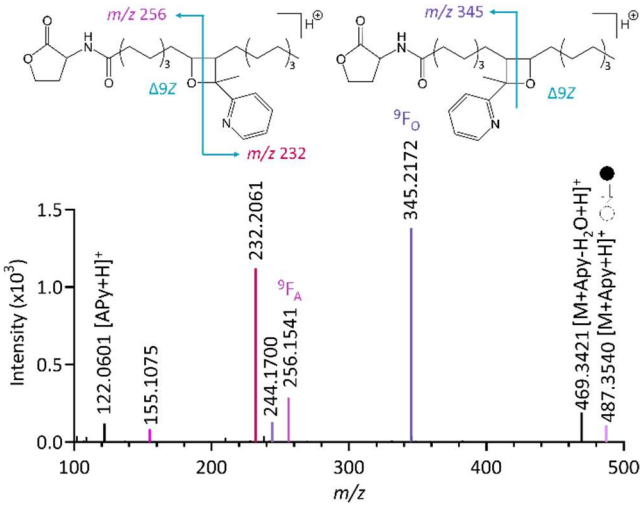

Fig. 2 CID-MS/MS spectrum of the Paternò-Büchi products (m/z_{exp} 487.3540, Δ_{error} = 2.1 ppm) of C18:1-Δ^9-*cis*-HSL (derivatization at 100 µM and analysis at 2.5 µM) after the in-solution derivatization using APy as reagent in acetonitrile after a 15-minute exposure at 254 nm. The MS/MS spectrum was obtained with a collision energy set at 15 eV.

3.2. Optimization of the Paternò-Büchi reaction in solution from the full factorial DOE

To assess the efficiency of Paternò-Büchi derivatization for AHLs, two key factors were considered: maximizing product intensity to achieve high-quality MS/MS spectra and minimizing potential side reactions. Relative amounts of Paternò–Büchi products (%^{PB}) and side products (%^{SP}) were evaluated to determine optimal conditions. Details on the calculation of %^{SP} and %^{PB} can be found in the supplementary information (section 5 and Fig. S8 to S10).A full factorial DOE was used to optimize the Paternò-Büchi conditions as it enables the simultaneous assessment of several parameters. As shown in Pareto charts available in Fig. S11, it was essential to take into account all parameters and parameter interactions for the optimization of the Paternò-Büchi derivatization. First, as previously explained (section 3.1), APy (λ_{max1}=227 nm, λ_{max2}=267 nm, Fig. S12) was undoubtedly the best reagent to localize the double bonds from AHL Paternò-Büchi products. As shown in Fig. 3, Paternò-Büchi products were obtained with APy, irrespective of the used AHL/reagent molar ratio, solvent or UV wavelength. It is worth noting that acetone is still the most commonly used reagent for the Paternò-Büchi reaction on other lipids [21, 32–34] even if other reagents [21, 22, 35–38] have also been used. However, acetone was not included as a reagent in our DOE as preliminary results showed no Paterno Buchi products between AHLs and acetone (Fig. S13).

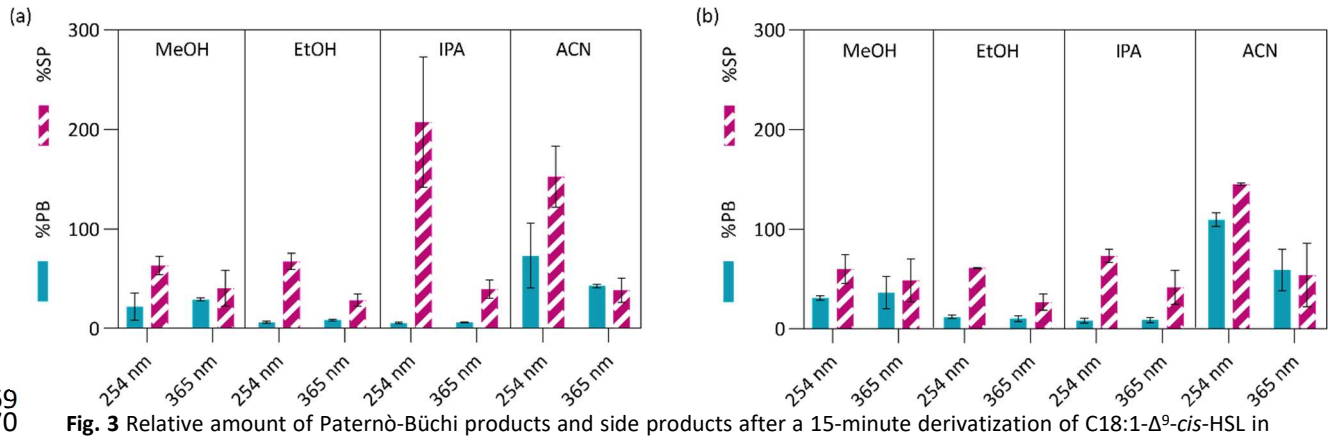

Fig. 3 Relative amount of Paternò-Büchi products and side products after a 15-minute derivatization of C18:1-Δ^9-*cis*-HSL in various solvents (methanol, ethanol, isopropanol and acetonitrile), using two UV lamps at different wavelengths (254 nm and 365 nm) and acetylpyridine at a AHL/reagent ratio of (a) 1/50 and (b) 1/100. Reactions were performed in triplicates (n=3) and samples were analyzed by LC-MS/MS.

As shown in Fig. 3, compared to protic solvents, acetonitrile yielded a higher quantity of Paternò-Büchi products due to the lower energy requirement for the carbonyl n → π* transition [39]. The choice of solvent and UV wavelength are correlated, with the optimal UV wavelength differing depending on the solvent. Acetonitrile at 254 nm was finally chosen to optimize the detection of Paternò-Büchi products. This result is consistent with previous finding on lipids from human plasma [37].

The AHL/APy molar ratio of 1/100 was determined as optimal, showing increased detection of Paternò-Büchi products while maintaing consistent side product levels across ratios of 1/20 to 1/200 (Fig. S14). However, beyond the 1/100 ratio, improvements in Paternò-Büchi products detection were not significant. Therefore, the optimal AHL/APy ratio was set at 1/100 to prevent source contamination with excess of APy.

3.3. Kinetic study

The optimal reaction time for maximizing Paternò-Büchi derivatization was determined through a kinetic study of the reaction between C18:1-Δ^9-*cis*-HSL (100 µM during the derivatization and 2.5 µM during the LC-MS/MS analysis) and APy (Fig. S15). $\%^{PB}$ increased over time, peaking at 15 min, before decreasing due to the formation of a higher proportion of unknown side products and potential retro-Paternò-Büchi reaction. Thus, a 15-minute derivatization time at 254 nm, in acetonitrile, and with APy at a AHL/reagent ratio of 1/100 was selected.

3.4. Stability studies

No clear degradation of the Paternò-Büchi products or side products was observed during 38 hours of storage at 6 °C (Fig. S16a) or after several freeze/thaw cycles as well (Fig. S16b). Therefore, derivatized samples can undergo extended LC sequences or multiple analyses without compromising the results. To our knowledge, this is the first stability study carried out on Paternò-Büchi products.

3.5. Paternò-Büchi derivatization of *Z/E* stereoisomers and AHLs with several double bonds

The MS/MS spectra of both *Z* and *E* stereoisomers exhibit similar patterns, indicating identical fragmentation of the resulting Paternò-Büchi products and ruling out stereochemical characterization of the double bond by this method (Fig. S17a and Fig. S17b). Additionally, Paternò-Büchi derivatization enables the localization of up to three double bonds on a single AHL, with no detection of multiple oxetane ring-containing products (Fig S17a and Fig. 4), suggesting that APy reacted with only one double bond at a time. Once more, the $^{X}F_{O}$ fragments consistently exhibited the highest intensity

across all AHL standards (Fig. 4 and Fig. S17), regardless of double bond position, stereochemistry, or number of unsaturations, thus confirming the annotation rule outlined in section 3.1.

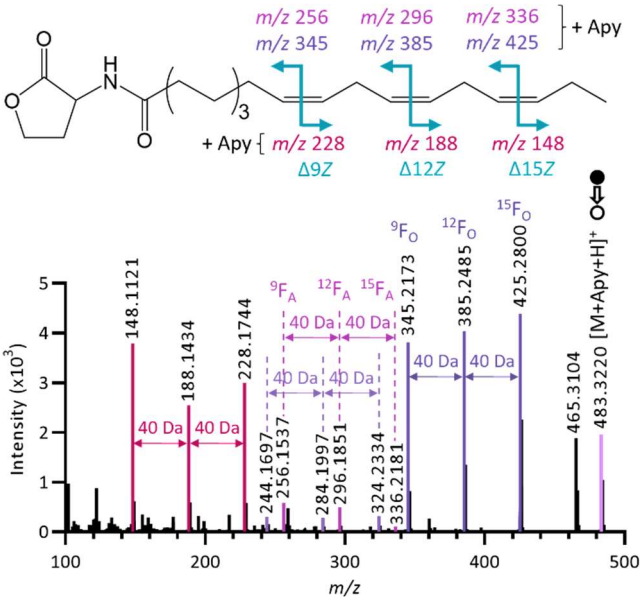

Fig. 4 CID MS/MS spectra of the Paternò-Büchi products of C18:3-$\Delta^{9,12,15}$-*cis*-HSL (m/z_{exp} 483.3220, Δ_{error} = 0.0 ppm) after in-solution derivatization using the APy reagent in acetonitrile after a 15-minute exposure at 254 nm. The MS/MS spectra were obtained with a collision energy set at 15 eV. All remaining fragments are annotated in Fig. S18.

3.6. Paternò-Büchi derivatization on bacterial extracts

3.6.1. Evaluation of the matrix effect

When extracting bacterial cultures with ethyl acetate, AHLs are typically mixed with other unsaturated specialized metabolites, potentially containing double bonds reactive with APy under UV irradiation [40, 41]. Additional experiments were conducted to evaluate the matrix effect on the previously developed method and adjust the AHL/APy molar ratio to account for the presence of other unsaturated compounds. For that purpose, C18:1-Δ^9-*cis*-HSL was added to the bacterial extract of the *Burkholderia* sp. BSNB-0181 strain where no unsaturated AHL was detected by LC-MS/MS. Two AHL concentrations were tested (2.5 µM and 25 µM) and three AHL/APy molar ratio were evaluated (1/100, 1/1000 and 1/10000). However, at the lowest AHL and APY concentrations (2.5 µM, 1/100 ratio, data not shown), most Paternò-Büchi products were below the limit of detection.

With the previous AHL/APy ratio of 1/100, the overall matrix effect induced a loss of at least 83 % of the Paternò-Büchi products peak areas ($ME\%^*$ below 17 %, Fig. S19a) while the ESI matrix effect led to a maximum loss of 26 % ($dME\%$ above 74 %, Fig. S19b), resulting in a maximum relative yield Y_{rel}^{PB} of 20 % for all AHL standards (Fig. S19c). Adjusting the APY/AHL ratio to 1/1000 increased the relative yield Y_{rel}^{PB} to between 26 % and 50 % (Fig. S19c), depending on the AHL standard and its initial concentration. However, further increasing the AHL/APy molar ratio to 1/10000 resulted in lower relative yields Y_{rel}^{PB} ranging between 18 % and 33 % (Fig. S19c). Therefore, the AHL/APy molar ratio of 1/1000 was selected for the derivatization of bacterial extracts.

3.6.2. Identification of AHLs and localization of C=C bonds in bacterial extract

As a proof of concept, the optimized Paternò-Büchi conditions were applied on the bacterial extract of the *Paraburkholderia tropica* BSNB-0562 strain. From the analysis of this bacterial extract prior

derivatization (Fig. 5a), a molecular network containing 411 nodes was generated (Fig. S20). As AHLs show similar fragmentation patterns including the loss of the lactone moiety (product ion at m/z_{theo} 102.0550) [30], the cluster of AHLs was easily located in the molecular network. From this cluster, seven AHLs, including two containing double bonds, were annotated (Table 1) by comparison of experimental $[M_{AHL}+ H]^+$ *m/z* values with a homemade database (Table S1) and retention times (when standards were available). Five AHLs were annotated as saturated as they matched with the database (Table S1).

After derivatization, double bonds of these two unsaturated AHLs (compound PB(7) and PB(8) in Fig 5b) were localized from the MS/MS spectra of Paternò-Büchi products, revealing OH-C16:1-Δ^9-HSL (compound 7, Fig. 5c) and oxo-C16:1-Δ^9-HSL (compound 8, Fig. 5d). After derivatization, as the Paternò-Büchi yield is not 100 %, both underivatized AHLs (compounds 7 and 8) were still detected (Fig 5b) and showed peak duplication. This duplication suggests the *Z/E* isomerization of C=C bonds during the UV exposure. The same trend was also observed when C18:1-Δ^9-*cis*-HSL and C18:1-Δ9-*trans*-HSL standards were derivatized (Fig S10), making it easier to detect AHLs containing double bonds.

The last two unknown AHLs were detected at 298.2016 (compound 3) and 296.1858 (compound 4). By comparison with the database (Table S1), compound 3 could be oxo-C12:1-HSL or OH-C12:2-HSL based on the $[M+H]^+$ *m/z* and compound 4 could be OH-C12:1-HSL based on the $[M+H]^+$ *m/z*. However, these two AHLs neither reacted with APy, nor showed *Z/E* isomerization (no duplication of peaks 3 and 4 in Fig 5b). This raised the question of their chemical structure, indicating that they do not contain any C=C double bond or that this double bond has a different reactivity towards the Paternò-Büchi and *Z/E* isomerization reactions in these optimized conditions (it may be an enone). Another hypothesis could be the presence of cyclic carbon-chains on AHLs. Even if it seems to be rare, unusual classes of AHL (such as coumaroyl-HSL) were previously reported [42]. Further investigations, including isolation, purification and full structural characterization by 2D-RMN, should be performed to conclude.

Table 1 Annotated AHLs produced by the *Paraburkholderia tropica* BSNB-0562 strain. *Compounds 3 and 4 are annotated as unknown AHL as they have the same $[M+H]^+$ *m/z* as respectively oxo-C12:1-HSL/OH-C12:2-HSL and OH-C12:1-HSL, but did not react with APy (no Paternò-Büchi products or peak duplication observed). One hypothesis is that these AHLs could be an enone or cyclic AHL.

Peak number	Annotated AHLs	Molecular formula	Theoretical $[M+H]^+$ *m/z*	Observed $[M+H]^+$ *m/z*	Δ_{error} (ppm)	Retention time (min)
1	OH-C8:0-HSL	$C_{12}H_{21}NO_4$	244.1543	244.1543	0.0	5.14
2	oxo-C8:0-HSL	$C_{12}H_{19}NO_4$	242.1387	242.1388	0.4	5.51
3	Unknown AHL*	$C_{16}H_{27}NO_4$	298.2013	298.2016	0.1	5.80
4	Unknown AHL*	$C_{16}H_{25}NO_4$	296.1856	296.1858	0.7	5.86
5	oxo-C10:0-HSL	$C_{14}H_{23}NO_4$	270.1700	270.1704	1.5	7.25
PB(7)	Paternò-Büchi products of OH-C16:1-Δ^9-HSL	$C_{27}H_{42}N_2O_5$	475.3166	475.3170	0.8	7.98
PB(8)	Paternò-Büchi products of oxo-C16:1-Δ^9-HSL	$C_{27}H_{40}N_2O_5$	473.3010	473.2988	4.6	7.52
6	oxo-C12:0-HSL	$C_{16}H_{27}NO_4$	298.2013	298.2013	0.0	8.65
7	OH-C16:1-Δ^9-HSL	$C_{20}H_{35}NO_4$	354.2639	354.2645	1.7	9.62
8	oxo-C16:1-Δ^9-HSL	$C_{20}H_{33}NO_4$	352.2482	352.2488	1.7	10.27
9	oxo-C16:0-HSL	$C_{20}H_{35}NO_4$	354.2639	354.2639	0.0	10.98

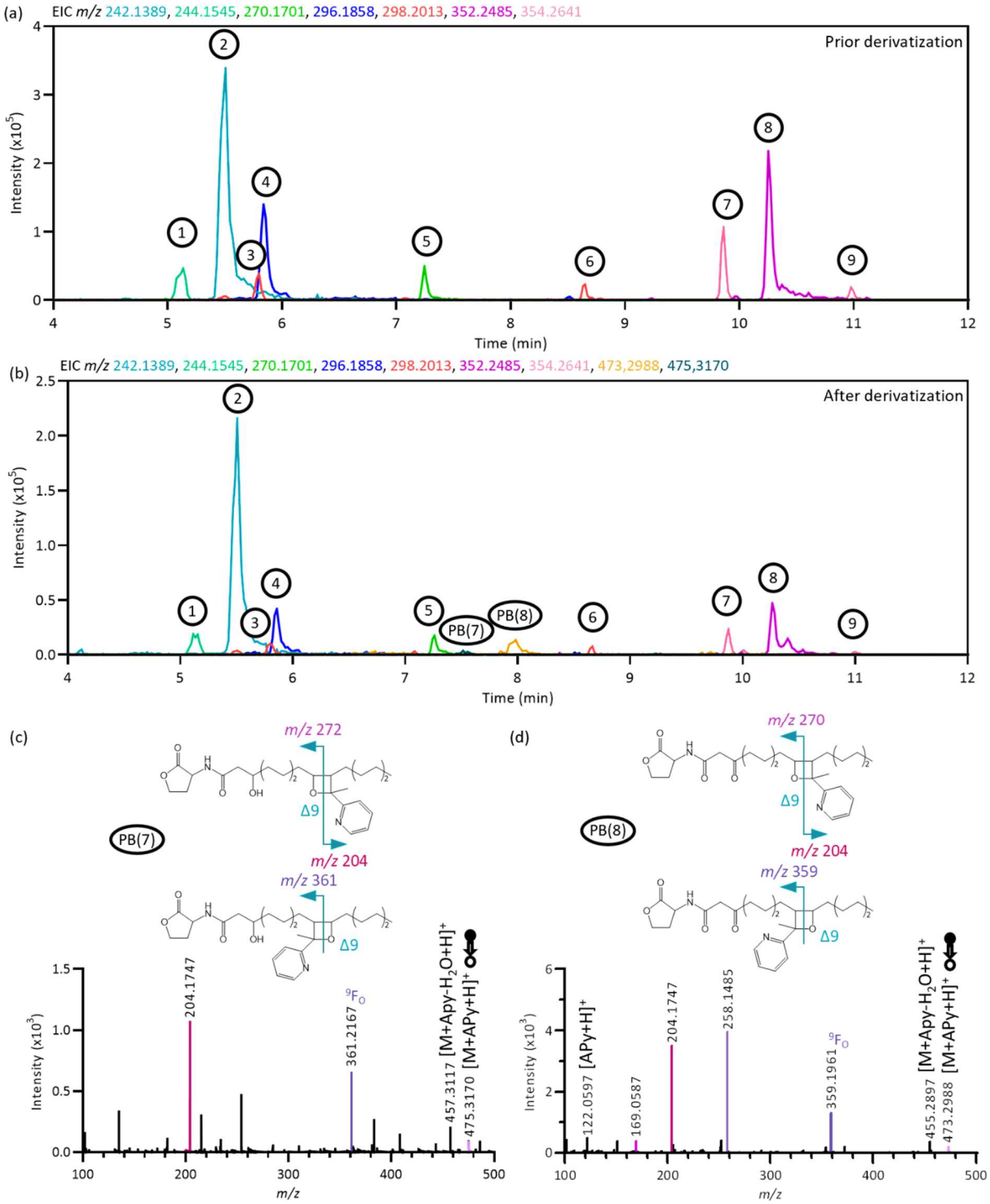

Fig. 5 Extracted ion chromatograms of all AHLs detected (a) prior derivatization and (b) after derivatization in the bacterial extract from the *Paraburkholderia tropica* BSNB-0562 strain (see Table 1 for peak identity). MS/MS spectra of the Paternò-Büchi products of (c) OH-C16:1-Δ9-HSL and (d) oxo-C16:1-Δ9-HSL. All remaining fragments are annotated in Fig. S21. The Paternò-Büchi derivatization was performed in acetonitrile using APy as reagent at AHL/APy molar ratio of 1/1000 during a 15-minute UV exposure at 254 nm.

The results obtained for this bacterial extract show that it is possible to use our optimized Paternò-Büchi conditions to localize the AHLs double bonds after the derivatization of the bacterial extract. This method could be used on other bacterial extracts of different strains or bacterial species.

4. Conclusion

We first optimized a method for the fine structural determination of AHLs, in particular to localize C=C bonds using Paternò-Büchi reaction in solution, directly from a diluted bacterial extract. In terms of analytical developments, it has been demonstrated that the Paternò-Büchi derivatization can be performed post-LC column on unsaturated phospholipids [43]. This method could then be implemented to characterize unsaturated AHLs in complex extracts taking into account that a large excess of APy is required (optimized to avoid as much as possible instrument contamination by a basic compound). For such post-LC column method, the reaction time could be lowered by optimizing the UV-transparent material used between the LC column to the MS. As AHLs are involved in bacterial communication and virulence, *in-situ* imaging on Petri dishes or biofilms on diverse surfaces after derivatization can be envisaged, as already described for phospholipids in biological tissues [44]. This may be particularly relevant as a diagnostic mean to detect molecular signatures in infectious bacteriology. On a more fundamental point of view, this method could be extended to tracking unsaturated long chains in metabolites.

5. CRediT authorship contribution statement

Clarisse Gosset-Erard: Methodology, Validation, Formal analysis, Investigation, Writing – original draft, Visualization. **Guanghui Han:** Resources, Writing – review & editing. **Dimitra Kyrko:** Investigation, Writing – review & editing. **Amandine Hueber:** Investigation, Supervision, Writing – review & editing. **Bastien Nay:** Conceptualization, Resources, Methodology, Writing – review & editing, Funding acquisition. **Véronique Eparvier:** Conceptualization, Resources, Methodology, Writing – review & editing, Funding acquisition. **David Touboul:** Conceptualization, Methodology, Writing – review & editing, Funding acquisition, Supervision.

6. Acknowledgements

This work was supported by a CHARM$_3$AT LabEx funding (postdoctoral fellowship of C. Gosset-Erard) and by the French ANR program (ANR-20-CE29-001). The authors would like to thank all the lab members, especially Salomé Poyer, for the fruitful discussions, Anaïs Demaye for her great help in the preparation of the bacterial extracts, Edith Nicol for her time and the access to a MALDI-FTICR-MS/MS used for preliminary analyses and the LAMBE laboratory for the access to the UV-vis spectrophotometer to acquire UV spectra of APy. The graphical abstract was created with Biorender.com.

7. Data availability

The datasets generated and analyzed during the current study are available from the corresponding author on request.

8. Conflicts of Interest

The authors declare that they have no known competing interests or personal relationships that could have appeared to influence the work reported in this paper.

9. References

1. Whiteley M, Diggle SP, Greenberg EP (2017) Progress in and promise of bacterial quorum sensing research. Nature 551:313–320. https://doi.org/10.1038/nature24624

2. Baltenneck J, Reverchon S, Hommais F (2021) Quorum Sensing Regulation in Phytopathogenic Bacteria. Microorganisms 9:239. https://doi.org/10.3390/microorganisms9020239

3. Kai K (2018) Bacterial quorum sensing in symbiotic and pathogenic relationships with hosts. Bioscience, Biotechnology, and Biochemistry 82:363–371. https://doi.org/10.1080/09168451.2018.1433992

4. Miller MB, Bassler BL (2001) Quorum sensing in bacteria. Annu Rev Microbiol 55:165–199. https://doi.org/10.1146/annurev.micro.55.1.165

5. Winson MK, Camara M, Latifi A, Foglino M, Chhabra SR, Daykin M, Bally M, Chapon V, Salmond GP, Bycroft BW (1995) Multiple N-acyl-L-homoserine lactone signal molecules regulate production of virulence determinants and secondary metabolites in *Pseudomonas aeruginosa*. PNAS 92:9427–9431

6. Suppiger A, Schmid N, Aguilar C, Pessi G, Eberl L (2013) Two quorum sensing systems control biofilm formation and virulence in members of the Burkholderia cepacia complex. Virulence 4:400–409. https://doi.org/10.4161/viru.25338

7. Kunakom S, Eustáquio AS (2019) *Burkholderia* as a Source of Natural Products. J Nat Prod 82:2018–2037. https://doi.org/10.1021/acs.jnatprod.8b01068

8. Reis VM, Santos PEL, Tenorio-Salgado S, Vogel J, Stoffels M, Guyon S, Mavingui P, Baldani VLD, Schmid M, Baldani JI, Balandreau J, Hartmann A, Caballero-Mellado J (2004) Burkholderia tropica sp. nov., a novel nitrogen-fixing, plant-associated bacterium. Int J Syst Evol Microbiol 54:2155–2162. https://doi.org/10.1099/ijs.0.02879-0

9. Naveed M, Hussain MB, Zahir ZA, Mitter B, Sessitsch A (2014) Drought stress amelioration in wheat through inoculation with Burkholderia phytofirmans strain PsJN. Plant Growth Regul 73:121–131. https://doi.org/10.1007/s10725-013-9874-8

10. Loong SK, Tan K-K, Zulkifle N-I, AbuBakar S (2019) Draft genome of *Paraburkholderia fungorum* sequence type 868 recovered from human synovial tissues. Data Br 25:104159. https://doi.org/10.1016/j.dib.2019.104159

11. Mahenthiralingam E, Vandamme P, Campbell ME, Henry DA, Gravelle AM, Wong LTK, Davidson AGF, Wilcox PG, Nakielna B, Speert DP (2001) Infection with Burkholderia cepacia Complex Genomovars in Patients with Cystic Fibrosis: Virulent Transmissible Strains of Genomovar III Can Replace Burkholderia multivorans. Clinical Infectious Diseases 33:1469–1475. https://doi.org/10.1086/322684

12. Fuqua C, Greenberg EP (2002) Listening in on bacteria: acyl-homoserine lactone signalling. Nat Rev Mol Cell Biol 3:685–695. https://doi.org/10.1038/nrm907

13. Churchill MEA, Chen L (2011) Structural Basis of Acyl-homoserine Lactone-Dependent Signaling. Chem Rev 111:68–85. https://doi.org/10.1021/cr1000817

14. Ziesche L, Wolter L, Wang H, Brinkhoff T, Pohlner M, Engelen B, Wagner-Döbler I, Schulz S (2018) An Unprecedented Medium-Chain Diunsaturated N-acylhomoserine Lactone from Marine Roseobacter Group Bacteria. Mar Drugs 17:20. https://doi.org/10.3390/md17010020

15. Ziesche L, Rinkel J, Dickschat JS, Schulz S (2018) Acyl-group specificity of AHL synthases involved in quorum-sensing in Roseobacter group bacteria. Beilstein J Org Chem 14:1309–1316. https://doi.org/10.3762/bjoc.14.112

16. Parsek MR, Val DL, Hanzelka BL, Cronan JE Jr, Greenberg EP (1999) Acyl homoserine-lactone quorum-sensing signal generation. Proc Natl Acad Sci USA 96:4360–4365

17. Horáček O, Portillo AE, Dhaubhadel U, Sung Y-S, Readel ER, Kučera R, Armstrong DW (2023) Comprehensive chiral GC-MS/MS and LC-MS/MS methods for identification and determination of N-acyl homoserine lactones. Talanta 253:123957. https://doi.org/10.1016/j.talanta.2022.123957

18. Rodrigues AMS, Lami R, Escoubeyrou K, Intertaglia L, Mazurek C, Doberva M, Pérez-Ferrer P, Stien D (2022) Straightforward N-Acyl Homoserine Lactone Discovery and Annotation by LC–MS/MS-based Molecular Networking. J Proteome Res 21:635–642. https://doi.org/10.1021/acs.jproteome.1c00849

19. Pham HT, Maccarone AT, Campbell JL, Mitchell TW, Blanksby SJ (2013) Ozone-Induced Dissociation of Conjugated Lipids Reveals Significant Reaction Rate Enhancements and Characteristic Odd-Electron Product Ions. J Am Soc Mass Spectrom 24:286–296. https://doi.org/10.1007/s13361-012-0521-9

20. Li H-F, Zhao J, Cao W, Zhang W, Xia Y, Ouyang Z (2022) Site-Specific Photochemical Reaction for Improved C=C Location Analysis of Unsaturated Lipids by Ultraviolet Photodissociation. Research 2022:. https://doi.org/10.34133/2022/9783602

21. Xu T, Pi Z, Song F, Liu S, Liu Z (2018) Benzophenone used as the photochemical reagent for pinpointing C=C locations in unsaturated lipids through shotgun and liquid chromatography-mass spectrometry approaches. Anal Chim Acta 1028:32–44. https://doi.org/10.1016/j.aca.2018.04.046

22. Zhao J, Xie X, Lin Q, Ma X, Su P, Xia Y (2020) Next-Generation Paternò–Büchi Reagents for Lipid Analysis by Mass Spectrometry. Anal Chem 92:13470–13477. https://doi.org/10.1021/acs.analchem.0c02896

23. Han G, Zhang W, Acs E, Paquin A, Ronzon Q, Casaretto N, Nay B (2024) Total Synthesis of Cyclotripeptidic Natural Products Anacine, Aurantiomide C, Polonimides A and C, and Verrucine F. Org Lett. https://doi.org/10.1021/acs.orglett.4c00658

24. Barthélemy M, Elie N, Pellissier L, Wolfender J-L, Stien D, Touboul D, Eparvier V (2019) Structural Identification of Antibacterial Lipids from Amazonian Palm Tree Endophytes through the Molecular Network Approach. IJMS 20:2006. https://doi.org/10.3390/ijms20082006

25. Nirma C, Eparvier V, Stien D (2015) Antibacterial Ilicicolinic Acids C and D and Ilicicolinal from *Neonectria discophora* SNB-CN63 Isolated from a Termite Nest. J Nat Prod 78:159–162. https://doi.org/10.1021/np500080m

26. Stinson CA, Xia Y (2016) A method of coupling the Paternò–Büchi reaction with direct infusion ESI-MS/MS for locating the C=C bond in glycerophospholipids. Analyst 141:3696–3704. https://doi.org/10.1039/C6AN00015K

27. Schmid R, Heuckeroth S, Korf A, Smirnov A, Myers O, Dyrlund TS, Bushuiev R, Murray KJ, Hoffmann N, Lu M, Sarvepalli A, Zhang Z, Fleischauer M, Dührkop K, Wesner M, Hoogstra SJ, Rudt E, Mokshyna O, Brungs C, Ponomarov K, Mutabdžija L, Damiani T, Pudney CJ, Earll M, Helmer PO, Fallon TR, Schulze T, Rivas-Ubach A, Bilbao A, Richter H, Nothias L-F, Wang M, Orešič M, Weng J-K, Böcker S, Jeibmann A, Hayen H, Karst U, Dorrestein PC, Petras D, Du X, Pluskal T (2023) Integrative analysis of multimodal mass spectrometry data in MZmine 3. Nat Biotechnol 41:447–449. https://doi.org/10.1038/s41587-023-01690-2

28. Olivon F, Elie N, Grelier G, Roussi F, Litaudon M, Touboul D (2018) MetGem Software for the Generation of Molecular Networks Based on the t-SNE Algorithm. Anal Chem 90:13900–13908. https://doi.org/10.1021/acs.analchem.8b03099

29. Elie N, Santerre C, Touboul D (2019) Generation of a Molecular Network from Electron Ionization Mass Spectrometry Data by Combining MZmine2 and MetGem Software. Anal Chem 91:11489–11492. https://doi.org/10.1021/acs.analchem.9b02802

30. Patel NM, Moore JD, Blackwell HE, Amador-Noguez D (2016) Identification of Unanticipated and Novel N-Acyl L-Homoserine Lactones (AHLs) Using a Sensitive Non-Targeted LC-MS/MS Method. PLoS ONE 11:e0163469. https://doi.org/10.1371/journal.pone.0163469

31. Rebane R, Oldekop M-L, Herodes K (2014) Matrix influence on derivatization and ionization processes during selenoamino acid liquid chromatography electrospray ionization mass spectrometric analysis. J Chromatogr B 955–956:34–41. https://doi.org/10.1016/j.jchromb.2014.02.016

32. Esch P, Heiles S (2020) Investigating C=C positions and hydroxylation sites in lipids using Paternò–Büchi functionalization mass spectrometry. Analyst 145:2256–2266. https://doi.org/10.1039/C9AN02260K

33. Zhu Y, Wang W, Yang Z (2020) Combining Mass Spectrometry with Paternò–Büchi Reaction to Determine Double-Bond Positions in Lipids at the Single-Cell Level. Anal Chem 92:11380–11387. https://doi.org/10.1021/acs.analchem.0c02245

34. Hu Q, Xia Y, Ma X (2021) Comprehensive Structural Characterization of Lipids by Coupling Paternò–Büchi Reaction and Tandem Mass Spectrometry. In: Hsu F-F (ed) Mass Spectrometry-Based Lipidomics: Methods and Protocols. Springer US, New York, pp 53–60

35. Cao W, Cheng S, Yang J, Feng J, Zhang W, Li Z, Chen Q, Xia Y, Ouyang Z, Ma X (2020) Large-scale lipid analysis with C=C location and sn-position isomer resolving power. Nat Commun 11:375. https://doi.org/10.1038/s41467-019-14180-4

36. Cerrato A, Capriotti AL, Cavaliere C, Montone CM, Piovesana S, Laganà A (2022) Novel Aza-Paternò-Büchi Reaction Allows Pinpointing Carbon–Carbon Double Bonds in Unsaturated Lipids by Higher Collisional Dissociation. Anal Chem 94:13117–13125. https://doi.org/10.1021/acs.analchem.2c02549

37. Zhao J, Fang M, Xia Y (2021) A liquid chromatography-mass spectrometry workflow for in-depth quantitation of fatty acid double bond location isomers. J Lipid Res 62:. https://doi.org/10.1016/j.jlr.2021.100110

528 38. Shi H, Tan Z, Guo X, Ren H, Wang S, Xia Y (2023) Visible-Light Paternò–Büchi Reaction for
529 Lipidomic Profiling at Detailed Structure Levels. Anal Chem 95:5117–5125.
530 https://doi.org/10.1021/acs.analchem.3c00085

531 39. Yabuno Y, Hiraga Y, Takagi R, Abe M (2011) Concentration and Temperature Dependency of
532 Regio- and Stereoselectivity in a Photochemical [2 + 2] Cycloaddition Reaction (the
533 Paternò−Büchi Reaction): Origin of the Hydroxy-Group Directivity. J Am Chem Soc 133:2592–
534 2604. https://doi.org/10.1021/ja1088524

535 40. Webster G, Jones C, Mullins AJ, Mahenthiralingam E (2020) A rapid screening method for the
536 detection of specialised metabolites from bacteria: Induction and suppression of metabolites
537 from Burkholderia species. J Microbiol Methods 178:106057.
538 https://doi.org/10.1016/j.mimet.2020.106057

539 41. Petrova YD, Mahenthiralingam E (2022) Discovery, mode of action and secretion of *Burkholderia*
540 sensu lato key antimicrobial specialised metabolites. The Cell Surface 8:100081.
541 https://doi.org/10.1016/j.tcsw.2022.100081

542 42. Yajima A (2016) Chapter 10 - Recent Advances in the Chemistry and Chemical Biology of Quorum-
543 Sensing Pheromones and Microbial Hormones. In: Atta-ur-Rahman (ed) Studies in Natural
544 Products Chemistry. Elsevier, pp 331–355

545 43. Zhang W, Zhang D, Chen Q, Wu J, Ouyang Z, Xia Y (2019) Online photochemical derivatization
546 enables comprehensive mass spectrometric analysis of unsaturated phospholipid isomers. Nat
547 Commun 10:79. https://doi.org/10.1038/s41467-018-07963-8

548 44. Chen Y, Xie C, Wang X, Cao G, Ru Y, Song Y, Iyaswamy A, Li M, Wang J, Cai Z (2022) 3-
549 Acetylpyridine On-Tissue Paternò–Büchi Derivatization Enabling High Coverage Lipid C═C
550 Location-Resolved MS Imaging in Biological Tissues. Anal Chem 94:15367–15376.
551 https://doi.org/10.1021/acs.analchem.2c03089

552